Journal of proteome research

Article

pubs.acs.org/jpr

Phosphoproteomics Reveals Resveratrol-Dependent Inhibition of Akt/mTORC1/S6K1 Signaling

Anya Alayev,[†,‡,⊥] Peter F. Doubleday,[§,⊥] Sara Malka Berger,[†] Bryan A. Ballif,*[,§] and Marina K. Holz*[,†,‡,∥]

[†]Department of Biology, Stern College for Women of Yeshiva University, New York, New York 10016, United States
[‡]Department of Molecular Pharmacology, Albert Einstein College of Medicine, New York, New York 10461, United States
[§]Department of Biology, University of Vermont, Burlington, Vermont 05405, United States
[∥]Albert Einstein Cancer Center, Albert Einstein College of Medicine, Bronx, New York 10461, United States

Supporting Information

ABSTRACT: Resveratrol, a plant-derived polyphenol, regulates many cellular processes, including cell proliferation, aging and autophagy. However, the molecular mechanisms of resveratrol action in cells are not completely understood. Intriguingly, resveratrol treatment of cells growing in nutrient-rich conditions induces autophagy, while acute resveratrol treatment of cells in a serum-deprived state inhibits autophagy. In this study, we performed a phosphoproteomic analysis after applying resveratrol to serum-starved cells with the goal of identifying the acute signaling events initiated by resveratrol in a serum-deprived state. We determined that resveratrol in serum-starved conditions reduces the phosphorylation of several proteins belonging to the mTORC1 signaling pathway, most significantly, PRAS40 at T246 and S183. Under these same conditions, we also found that resveratrol altered the phosphorylation of several proteins involved in various biological processes, most notably transcriptional modulators, represented by p53, FOXA1, and AATF. Together these data provide a more comprehensive view of both the spectrum of phosphoproteins upon which resveratrol acts as well as the potential mechanisms by which it inhibits autophagy in serum-deprived cells.

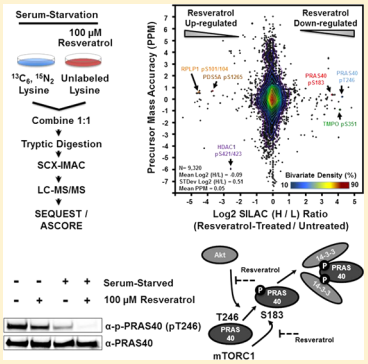

KEYWORDS: *mTORC1, resveratrol, S6K1, PRAS40, SILAC, phosphoproteomics*

INTRODUCTION

Resveratrol (*trans*-3,5,4′-trihydroxystilbene), a polyphenol naturally found in grapes, peanuts and red wine, possesses disease-protective and antiaging properties.[1] It has been studied as a chemo-preventative and antitumor agent, and has been investigated for lifespan-extending and disease-suppressing properties. On a cellular level, resveratrol exhibits pleiotropic effects, yet, its antiaging properties have been directly linked to the activation of sirtuins, namely, Sirt 1 (a class II histone deacetylase)[2] and to the regulation nutrient- and energy-sensing pathways via the activation of AMPK.[3] Several groups, including ours, have demonstrated that under different cellular contexts resveratrol has the ability to increase or decrease autophagy, a conserved catabolic process responsible for the bulk degradation of proteins and organelles. Induced by nutrient- and serum-deprivation, autophagy allows cells to survive under metabolic stress. However, the process can also result in cell death.[4−6] Furthermore, long-term reseveratrol treatment in nutrient-rich conditions induces autophagy, while acute treatment under starvation conditions inhibits autophagy.[4] The induction of resveratrol-dependent autophagy is independent of Sirt1 and is rather mediated via the mechanistic target of rapamycin complex 1 (mTORC1)/S6 kinase 1 (S6K1) signaling pathway.[4]

mTOR, a serine/threonine kinase that belongs to the phosphatidylinositol 3-kinase-related kinase (PIKK) family, was discovered as a target of a naturally occurring bacterial macrolide rapamycin. mTOR interacts with regulatory proteins to form two different complexes: mTORC1 and mTORC2. These complexes differ in their protein composition, downstream targets, and sensitivity to rapamycin, with mTORC1 being acutely rapamycin-sensitive and mTORC2 being acutely rapamycin-insensitive.[7,8] In response to extracellular signals such as nutrient availability and growth factors, mTORC1 signaling regulates numerous metabolic functions, including protein, nucleotide and lipid synthesis.[9,10] Furthermore, mTORC1 activation down-regulates AMPK by increasing amino acid uptake[11] and reduces ULK1 activity, potently inhibiting autophagy resulting in increased cell growth and proliferation.[8] Conversely, inhibition of mTORC1 by rapamycin phenocopies nutrient-deprivation and potently induces autophagy.[12] In addition, in yeast resveratrol can suppress autophagy induced by rapamycin.[4] This provides some measure of paradox as both rapamycin and resveratrol inhibit S6K.[4] Given this paradox and given that resveratrol is a promising compound in the prevention and treatment of age-related

Received: July 8, 2014
Published: October 13, 2014

diseases including cancer,[3,13] there exists a need to better understand its mechanism of action. Therefore, we performed a phosphoproteomic analysis focused on identifying potential effectors of autophagy that are regulated by acute resveratrol treatment in serum-deprived cells.

EXPERIMENTAL PROCEDURES

Cell Culture and Treatments

For non-SILAC experiments, cells were cultured in Dulbecco's Modified Eagle's Medium (DMEM) containing 10% fetal bovine serum (FBS, Hyclone, Logan, UT), 50 units/mL penicillin, and 50 μg/mL streptomycin in a humidified incubator with 5% CO_2 at 37 °C.

For SILAC experiments, cells were grown in DMEM prepared deficient in L-arginine and L-lysine (Thermo Fisher Scientific, Inc., Rockford, IL), and supplemented with 10% dialyzed fetal bovine serum (Hyclone); 50 units/mL penicillin and 50 μg/mL streptomycin; 42 mg/L unlabeled L-arginine; and either 73 mg/L unlabeled L-lysine for light samples, or 73 mg/L $^{13}C_6$-, $^{15}N_2$-L-lysine (Cambridge Isotope Laboratories, Inc., Andover, MA) for heavy samples. Cells grown in 10% FBS were treated for 30 min with 20 nM rapamycin (Sigma-Aldrich, St. Louis, MO) and, or in addition to, 50 or 100 μM resveratrol (Sigma-Aldrich), while cells grown under nutrient deprived conditions were treated with 50 μM resveratrol for 30 min.

Immunoblots

Following treatment, cells were lysed in ice-cold lysis buffer (10 mM KPO_4 (pH 7.3), 1 mM EDTA, 10 mM $MgCl_2$, 50 mM β-glycerophosphate, 5 mM EGTA, 0.5% Nonidet P-40 (NP-40), 0.1% Brij 35, 1 mM sodium orthovanadate, 40 μg/mL phenylmethylsulfonyl fluoride, 10 μg/mL leupeptin, 5 μg/mL pepstatin A). Lysates were cleared of insoluble material by centrifugation at 15 000*g* for 10 min at 4 °C. Protein concentrations in cell extracts were measured by Bradford assays (Bio-Rad, Hercules, CA) according to the manufacturer's protocol using an Eppendorf BioPhotometer. Samples were equalized for protein concentration and denatured using 4× NuPAGE LDS Sample buffer and 10× Reducing agent (Invitrogen, Carlsbad, CA) at 70 °C for 10 min. Samples were resolved using Bis-Tris Plus gels (Invitrogen) and transferred onto nitrocellulose membrane (GE Healthcare, Rahway, NJ). Membranes were probed with the following primary antibodies: p-PDK1 (pSer241), PDK1, p-Akt (pSer473), Akt, p-S6K1 (pThr389), p-S6K1 (pThr421/424), p-S6K1 (pSer371), S6K1, p-eIF4B (pSer422), eIF4B, p-S6 (pSer240/244), S6, p-PRAS40 (pThr246), p-PRAS40 (Ser183), PRAS40, p4E-BP1 (pSer65), 4EBP1, p62/SQSTM1, pERK1/2 (T202, Y204), ERK1/2 (above antibodies from Cell Signaling Technology, Danvers, MA), and actin (Santa Cruz Biotechnology, Dallas, TX). Blots were incubated with IRDye-conjugated anti-rabbit, anti-mouse or anti-goat secondary antibodies (LI-COR, Lincoln, NE) and imaged using an Odyssey Infrared detection instrument (LI-COR). All immunoblots were performed at least thrice to ensure reproducibility.

Peptide Preparation

Cellular pellets from each biological replicate were resuspended in urea lysis buffer (8 M urea, 100 mM NaCl, 25 mM Tris-HCl (pH 8.0), 25 mM NaF, 10 mM $Na_4P_2O_7$, 1 mM Na_3VO_4, 50 mM β-glycerophosphate, 1 mM PMSF, 10 μg/mL leupeptin, 5 μg/mL pepstatin A) and sonicated for three, 1 min intervals at 4 °C on a Kontes 50 W sonicating microprobe tip (Kontes Co., Vineland, NJ) at 50% duty output. Insoluble debris was then spun down by centrifugation for 30 min at 15 000*g*. Dithothreitol (DTT) was added to 5 mM and the clarified lysate was reduced at 56 °C for 40 min. Cooled samples were then alkylated with 14 mM iodoacetamide for 1 h in the dark.

After a 1:4 dilution in 25 mM Tris-HCl (pH 8.0), proteins were digested with the addition of sequencing-grade modified trypsin (Promega, Madison, WI) at 1:100 (μg trypsin/μg protein) overnight at 37 °C. Following digestion, the samples were acidified by adding trifluoroacetic acid (TFA) to 0.4%. Insoluble material was then removed from the digest via centrifugation at 4000*g* for 20 min at 4 °C. The supernatants from biological replicates were separately desalted on Waters (Waters Corporation, Milford, MA) tC18 columns (preconditioned by an initial treatment with 100% acetonitrile (MeCN) and then equilibrated with 0.1% trifluoroacetic acid (TFA)), and washed with 0.1% TFA, 2.5% MeCN, and then peptides were eluted with 40% acetonitrile, 0.1% TFA, and dried via lyophilization prior to phosphopeptide enrichment.

SCX Chromatography

Dried peptides were resuspended in 7 mM KH_2PO_4, 33% MeCN, and applied to preconditioned polySULPHOETHYL A columns (PolyLC Inc., Columbia, MD). Elutions were collected as fractions in 0, 4, 8, 12, 20, 45, 90, and 250 mM KCl in resuspension buffer. Fractions were dried via lyophilization and resuspended in 0.1% TFA for desalting on tC18 columns as described above.

IMAC Enrichment

Desalted peptides from each SCX fraction were resuspended in 100 μL of 40% MeCN, 25 mM formic acid (FA). To each sample was added 40 μL of a 50% slurry of PHOS-Select IMAC resin (Sigma-Aldrich) and vigorously shaken on a vortex unit fit with a tube-holding attachment for 1 h at room temperature. An additional 50 μL of resuspension buffer was added to each fraction, and samples were loaded onto homemade crimped, 200 μL gel-loading tips as described previously.[14] The flowthrough was collected and reapplied to the IMAC resin three times prior to washing twice with 120 μL of resuspension buffer. Phosphopeptides were eluted with 50 mM K_2HPO_4 (pH 10), and the samples were neutralized with 10% FA. Peptides were dried in a speed vacuum.

LC–MS/MS and Data Analysis

Dried peptides were suspended in 2.5% MeCN, 2.5% FA and were loaded for nanoscale microcapillary LC–MS/MS in a LTQ-Orbitrap mass spectrometer (Thermo Electron, Waltham, MA) fitted to a Finnigan Nanospray II electrospray ionization source, a Surveyor HPLC pump plus, and a Micro AS autosampler (all from Thermo Electron) as described.[15] Briefly, after an isocratic loading for 15 min in solvent A (2.5% MeCN, 0.15% FA), peptides were separated on an increasing MeCN gradient (2.5–35%) containing 0.15% FA from 15 to 60 min on a 100 μm internal diameter, in-house prepared, 13 cm long, MagicC18 reverse phase column (5 μm, 200 Å; Michrom Bioresources, Auburn, CA) with a needle tip diameter of ~4.5 μm. Data acquisition was done in a top-10 format with a precursor scan (365–2000 m/z) followed by 10 data-dependent MS/MS scans. Dynamic exclusion was enabled with a repeat count of 3 and a repeat cycle of 120 s. Lock mass was enabled and set to calibrate on the mass of a polydimethylcyclosiloxane ion $[(Si(CH_3)_2O)_5 + H^+]^+$, m/z =

dx.doi.org/10.1021/pr500714a | J. Proteome Res. 2014, 13, 5734–5742

371.10120. The precursor parts per million (ppm) values were adjusted slightly based on the average ppm values for the peptides identified at a less than 0.5% false discovery rate in each run (see below).

Mass spectra were searched using SEQUEST (Thermo Electron V26.12) against the human forward and reverse concatenated IPI database (human IPI v3.60) using a target-decoy approach[16] and allowing for variable phosphorylation of serine, threonine and tyrosine (+79.96633 Da), oxidation of methionine (+15.99429), carbamiodomethylation of cysteine (+57.02146 Da), and heavy-labeled lysine (+8.0141988132.). Peptide quantification was performed using Vista-based software[17,18] taking the integral values of the chromatographic monoisotopic peaks generated from full MS1 scans. MS runs were pooled by biological replicate and filtered below a 0.5% false discovery rate using an automated linear discriminant analysis[19] weighted by XCorr, ΔCn2, MS2 ion intensity, missed tryptic cleavages, precursor ppm and peptide length. The Ascore algorithm[20] was employed to assess ambiguity in phosphorylation site localization.

Bioinformatics

The DAVID bioinformatics resource[21,22] was utilized to examine gene ontology and identify enriched biological processes. Enrichment was assessed through the *p*-values provided by the bioinformatics analyses.

RESULTS AND DISCUSSION

Resveratrol Prevents Autophagy Induction by Serum Starvation

We first tested the effect of resveratrol on autophagy as a function of serum in MCF7 adenocarcinoma-derived cells. MCF7 cells were used because they have a high-copy amplification of the gene encoding S6K1, resulting in high levels of S6K1 expression and activity. We reasoned that this might allow for enrichment of putative S6K1 target substrates whose perturbation by resveratrol might be more readily observed.[23] We detected that the addition of resveratrol to cells growing in full serum resulted in a decrease in p62/SQSTM1 levels, consistent with an increase in autophagy.[24,25] In contrast, serum starvation resulted in lower p62/SQSTM1 levels, yet this decrease was blocked by the addition of resveratrol (Figure 1A). This suggested that our MCF7 cell culture model provided an opportunity to identify resveratrol targets capable of regulating autophagy in serum-starved conditions.

The Effects of Resveratrol on the Phosphoproteome

Because the ability of resveratrol to inhibit autophagy has been shown to be mediated via the mTORC1/S6K1 signaling pathway, we next examined the effects of acute treatment of MCF7 cells with resveratrol on the phosphorylation of potential S6K1 target proteins. We used the anti-(RX)-RXXpS/T antibody that recognizes the consensus phosphorylation motif of the AGC-family of kinases that includes S6K1, and consists of phosphorylation of serine or threonine preceded by arginine at positions −5 and most importantly at −3. When MCF7 cells were treated with resveratrol in the presence of serum, we observed dose-dependent reduction in the phosphorylation of several proteins. However, resveratrol alone was not as effective as rapamycin in reducing protein phosphorylation under these conditions, as evidenced by the levels of phospho-S6, the canonical S6K1 target protein (Figure 1B). We also tested the ability of resveratrol to inhibit generic

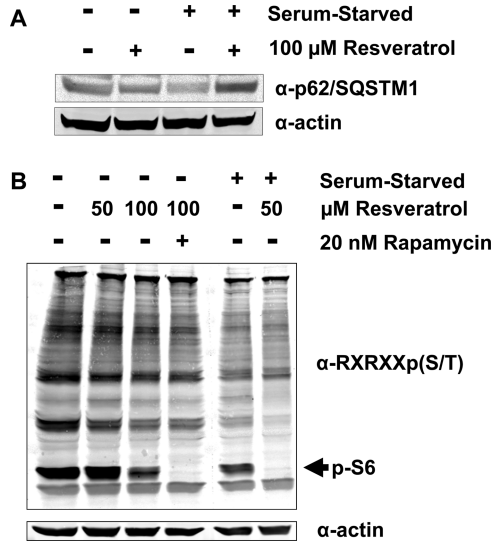

Figure 1. The effect of resveratrol on an autophagy marker and anti-RXRXXpS/T reactivity in full serum and serum-deprived conditions. (A) Resveratrol prevents autophagy induction by serum starvation as measured by p62/SQSTM1 levels. MCF7 cells were grown in media containing either 10% FBS or 0% FBS (serum-starved) and treated with the indicated concentration of resveratrol for 24 h. Cells were lysed and the indicated proteins were detected by immunoblot. (B) The effect of resveratrol on anti-RXRXXpS/T reactivity in full serum and serum-deprived conditions. MCF7 cells were grown in media containing either 10% FBS or 0% FBS (serum-starved). Cells grown in 10% FBS were treated with the indicated concentrations of resveratrol for 30 min. In the case of Rapamycin treatment, cells were subjected to 20 nM Rapamycin overnight before the 30 min Resveratrol treatment. Cells grown in 0% FBS overnight were treated with 50 μM Resveratrol for 30 min. Cells were lysed and the indicated proteins were detected by immunoblot.

AGC kinase substrate phosphorylation in the absence of serum. In serum-deprived cells, resveratrol potently inhibited basal phosphorylation of S6, and reduced phosphorylation of several other putative AGC family targets. These data suggested that under conditions of serum-deprivation resveratrol might be more distinguishable as a modulator of S6K1 signaling. Taken together, the results shown in Figure 1 suggested our cell culture system might enable us to identify resveratrol-inhibited targets of S6K1/AGC kinases with the potential to reduce autophagy under serum-starved conditions. Therefore, we performed a phosphoproteomic analysis of MCF7 cells under serum-starved conditions to identify proteins targeted for reversible phosphorylation by resveratrol.

Characterization of the Resveratrol-Regulated Phosphoproteome

To investigate global changes in phosphorylation under serum-deprived conditions and following acute resveratrol treatment, we metabolically labeled MCF7 cells using stable isotope labeling with amino acids in cell culture (SILAC).[26] In this case, SILAC would permit relative mass spectrometry-based quantification of phosphopeptides from cells grown in two serum-starved states (with or without resveratrol) based on differential-labeling using amino acids with or without ^{13}C and ^{15}N. Heavy-labeled cells were left untreated, whereas unlabeled cells were treated with 100 μM resveratrol for 30 min. Cellular extracts from two biological replicates were independently subjected to an established phosphopeptide-enrichment workflow based on HPLC-independent SCX-IMAC fractionation

dx.doi.org/10.1021/pr500714a | J. Proteome Res. 2014, 13, 5734−5742

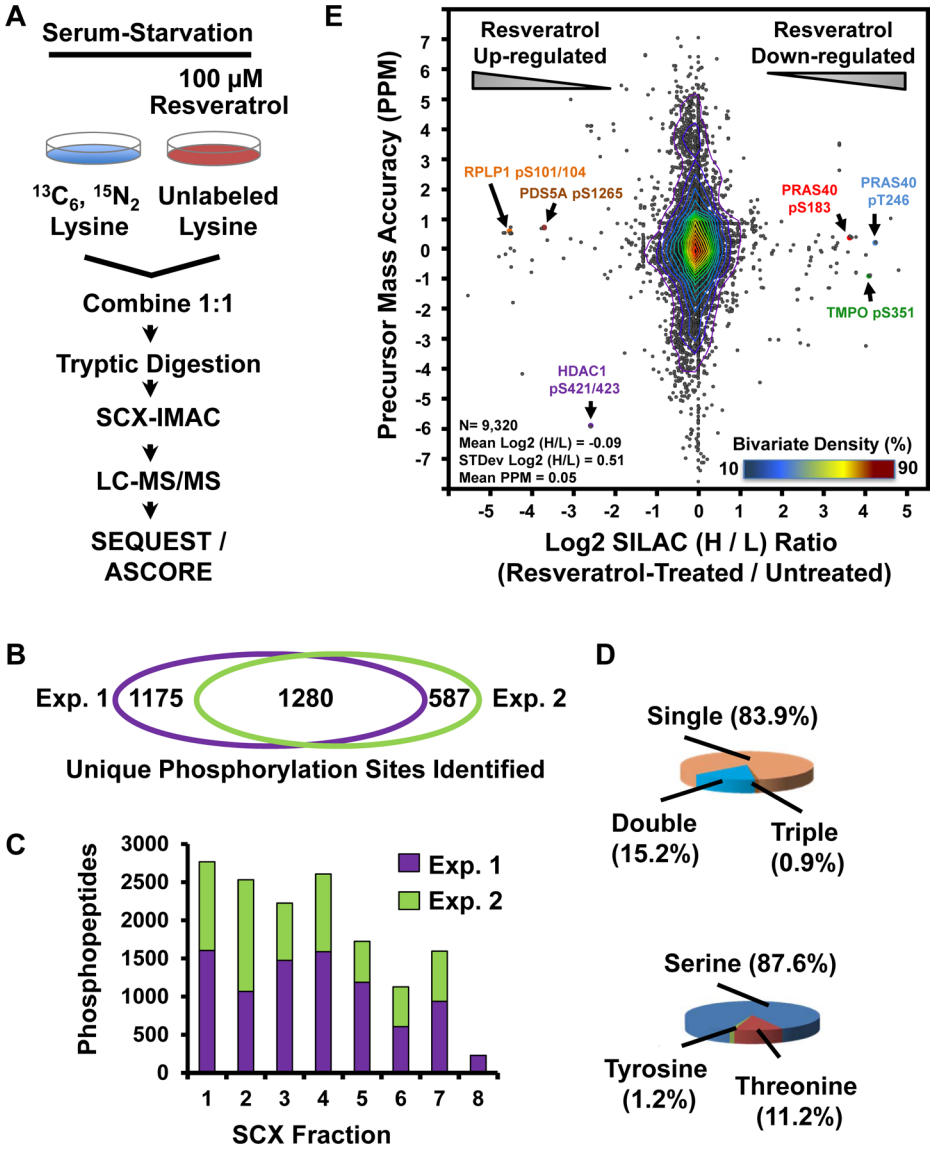

Figure 2. Phosphoproteomic analysis of serum-starved, resveratrol-treated MCF7 cells. (A) Workflow to discover Resveratrol-induced dynamic phosphorylation events. MCF7 cells were metabolically labeled with SILAC media, were serum-starved overnight (light), and treated with 100 μM Resveratrol for 30 min, or serum starved alone (heavy). Cells were harvested and combined at a 1:1 ratio, homogenized by urea lysis and sonication, and trypsinized. Desalted peptides were subjected to SCX-IMAC and enriched phosphopeptide-fractions were analyzed by LC–MS/MS. The SEQUEST algorithm and Ascore were used for identification of and confident site localization of post-translational modifications, respectively. (B) Venn Diagram showing unique phosphorylation sites identified from biological replicates. (C) Biological replicates showed similar numbers of phosphopeptides identified from each of the eight strong-cation exchange fractions. (D) Distribution of phosphopeptides by number of phosphorylation sites per tryptic peptide and amino acid residue. (E) Bivariate density analysis plotting the measured mass accuracy of the precursor phosphopeptide ions (in ppm) with their Log2 H/L SILAC ratios. All identified phosphopeptides from the two biological replicates were plotted. Indicated are resveratrol-upregulated and -downregulated phosphopeptides with selected sites highlighted. The data inside of the lowest bivariate density curve represents 90% of all phosphopeptides, with minor lines corresponding to 5% density differences.

and liquid-chromatography tandem mass spectrometry using a linear ion trap-orbitrap hybrid mass spectrometer (Figure 2A).[15,27] We conducted SEQUEST searches using a target-decoy search[16] to below a 0.5% false discovery rate. All resultant phosphopeptides fell into a precursor mass window of ±8 ppm with a mean mass error of only 0.50 ppm (Supporting Information Tables 1 and 2).

From our large-scale SILAC approach, we confidently identified 16399 phosphopeptides, yielding 3042 unique phosphorylation sites from 1289 proteins under serum-starved and resveratrol-treated conditions. A total of 1280 unique phosphorylation sites were common to the two biological replicates (Figure 2B, Supporting Information Tables 1 and 2). The biological replicates yielded similar numbers of phosphopeptides across salt-bumps in the SCX chromatography (Figure 2C). A majority of identified phosphopeptides were singly phosphorylated (83.9%), while 15.2% were doubly phosphorylated and 0.9% were triply phosphorylated (Figure 2D). Consistent with the cellular proportions of phosphorylated amino acids,[28,29] 87.6% of identified peptides contained phosphoserine, while 11.2% contained phosphothreonine, and 1.2% contained phosphotyrosine (Figure 2D).

Given the Western blotting results in Figure 1, and given signaling pathways were generally suppressed due to depriving

dx.doi.org/10.1021/pr500714a | J. Proteome Res. 2014, 13, 5734–5742

the cells of serum prior to resveratrol treatment, we expected that the majority of phosphorylation sites would exhibit a limited quantitative response between resveratrol and control conditions. Indeed, combining both biological replicates into one data set, 90% of all quantifiable phosphopeptides (9320) fell within a 2-fold quantitative change with a mean Log2 (H/L) quantification of −0.091 and a standard deviation of only ±0.51 (Figure 2E, Supporting Information Figure 1). As shown in a bivariate (ppm versus Log2 (H/L)) density plot of all quantified phosphopeptides, only a limited subset of phosphorylation sites exhibited a significant response to resveratrol treatment (Figure 2E).

To assess the reproducibility of quantification between biological replicates, we compared their phosphopeptide quantification distributions. The first biological replicate had a mean Log2 (H/L) ratio of −0.07 and a standard deviation of ±0.52. The second biological replicate had a mean Log2 (H/L) ratio of −0.12 and a standard deviation of ±0.49. The distribution in quantification of phosphopeptides was also strikingly similar (Supporting Information Figure 1A). Furthermore, as mentioned above, a similar number of phosphopeptides were identified in each strong-cation exchange fraction between biological replicates (Figure 2C).

We also investigated phosphorylation changes occurring at the protein level, and grouped peptides by their IPI accessions to generate a mean quantification and standard deviation for each phosphoprotein. This was done by creating a mean SILAC ratio from the means of all phosphorylation sites identified for a given protein. It is understood that many proteins have unique phosphorylation sites that show inverse relationships in their degrees of phosphorylation in order to achieve a given state of activity. This complexity, however, is likely to be reduced given the analysis was conducted under serum-starved conditions. We gave each protein equal weight, independent of the number of spectra contributing to its identification in order to give lower abundance phosphoproteins better representation. Similar to peptide-level changes, the resultant quantile plot showed normally distributed phosphoproteins with the grand mean Log2 (H/L) ratio of 0.03, and a standard deviation of 0.43 (Supporting Information Figure 1B).

Analysis of PI3K/mTOR Signaling in Response to Resveratrol Treatment

Given the established roles of proteins in the mTORC1/S6K1 pathway in processes known to be regulated by resveratrol, we first examined the data set for resveratrol-induced changes in the phosphorylation of proteins in this signaling pathway. Interestingly, we found that resveratrol had little effect on the identified phosphorylation sites found on the majority of mTORC1/S6K1-regulated signaling proteins, including the protein kinase ULK1, a critical regulator of autophagy.[30] Indeed, two mTOR-regulated sites on ULK1, Ser638 and Ser639[31] did not change significantly (Supporting Information Table 1). However, it may be that the acute addition of resveratrol does not affect ULK1-dependent autophagy at this time point but exhibits mechanistic consequences at later times. We expect, for example, that 30 min of resveratrol treatment under serum-starved conditions is not yet sufficient to observe changes in ULK1 phosphorylation, and that our screen would be facilitating phosphorylation changes very proximal to resveratrol targets. However, there was a striking effect of resveratrol on the phosphorylation PRAS40. Two sites, T246 and S183, were observed to be dramatically down-regulated by resveratrol. T246 of PRAS40 has been best characterized as an Akt phosphorylation site, and S183 is best understood to be a mTORC1 phosphorylation site.[32,33] Phosphorylation of these sites, most notably T246, leads to the dissociation of PRAS40 with mTORC1[34] and its subsequent interaction with 14-3-3.[33] Furthermore, PRAS40 dissociation from mTORC1 correlates with increased 4E-BP1 binding to mTORC1[34] via RAPTOR.[35] Active mTORC1 phosphorylates 4E-BP1 which then dissociates from eIF4E and enables it to participate in 5′ cap-dependent translation.[35,36]

We orthogonally validated some of the proteomics data by immunoblotting with phosphorylation site-specific antibodies. Consistent with the phosphoproteomic data, PRAS40 phosphorylation at T246 showed a dramatic decrease upon treatment of starved cells with resveratrol (Figure 3).

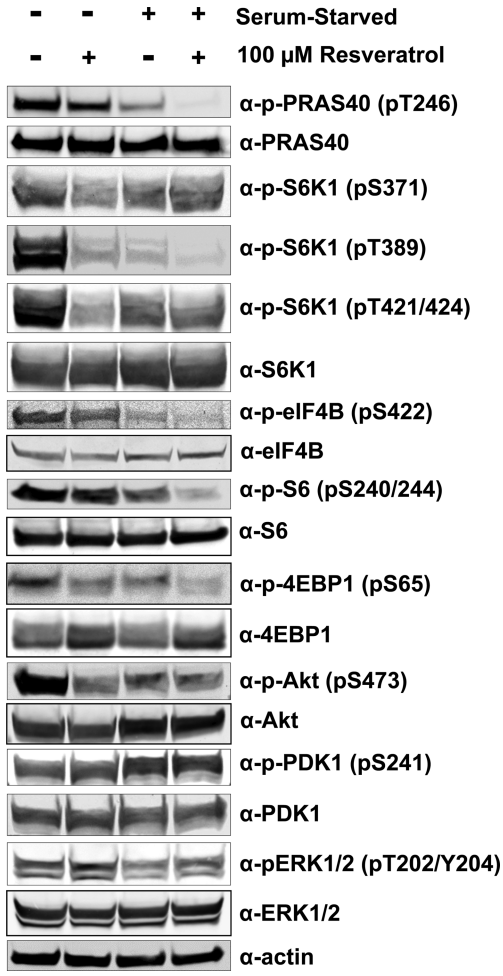

Figure 3. Validation of phosphorylation sites related to PI3K/mTORC1 signaling. MCF7 cells were grown in media with or without 10% FBS for 24 h and subsequently treated with 100 μM Resveratrol for 30 min. Cells were lysed, and the indicated proteins were detected by immunoblot.

Additional consistencies were observed with S6K1 pT389 showing a slight reduction with resveratrol treatment and other phospho-specific probes showing little to no change (Figure 3). Phosphorylation of S6K1 at Thr389 correlates with its kinase activity and is largely mediated by mTORC1, indicating that resveratrol inhibits S6K1 signaling, perhaps through lowering mTORC1 activity toward specific substrates. We also detected

dx.doi.org/10.1021/pr500714a | J. Proteome Res. 2014, 13, 5734−5742

reduction in phosphorylation of 4E-BP1, another target of mTORC1 activity. Resveratrol also inhibited phosphorylation of two direct protein targets of S6K1, eIF4B at Ser422 and S6 at Ser240/244 (Figure 3), further validating previously established inhibition of this pathway.[4] However, we also noted some surprising differences in the proposed mechanism of regulation of this pathway upstream of mTORC1. Although work from other groups has indicated that resveratrol is able to inhibit PI3K and its downstream signaling,[37] we did not find significant effects on PI3K signaling other than the negative regulation of PRAS40 T246 phosphorylation (presumably by Akt) under the serum-deprived conditions employed in our study. Of note, however, is that AGC kinases share target specificities and therefore it is possible that some measure of PRAS40 T246 phosphorylation could be happening via other AGC kinases (e.g., S6K). This is a research avenue that we are currently pursuing. Resveratrol did not have a significant effect on phosphorylation of PDK1, in accord with previous reports demonstrating constitutive PDK1 activation loop phosphorylation.[38] Moreover, resveratrol treatment downregulated phosphorylation of Akt at Ser473 in serum containing media, but little effect was observed in serum-deprived conditions (Figure 3). It is possible, however, that under serum-starved conditions the baseline reactivity of true signal for the pSer473 Akt antibody cannot easily be distinguished above the antibody's reactivity with Akt nonspecifically. Future studies will examine the effect of resveratrol on Akt kinase activity under serum-starved conditions.

Bioinformatic Analysis of Resveratrol-Regulated Processes Reveals mTORC1/S6K1 and Chromatin Remodeling/Transcription as Major Targets

To assess biological processes altered under resveratrol treatment, proteins with at least one phosphorylation site and a quantification value greater than one standard deviation from the mean were subjected to bioinformatic analysis using the DAVID bioinformatics portal. As phosphorylation and its regulation are dynamic in manifesting biological responses, we grouped resveratrol-upregulated and resveratrol-downregulated sites to one list giving a greater foreground list of genes to identify GO enrichments. In widening possible outcomes, we also set a relatively stringent cutoff for GO enrichment. Given the minimum enrichment score produced by DAVID as a function of p-value, $-\mathrm{Log}(p\text{-value}) = 1$, we employed a log-transformed p-value cutoff of 2.5 to filter out low scoring terms. Under these parameters, 21 GO terms were identified as significantly enriched including chromosome organization, mRNA processing and transcriptional activities as major enrichments (Figure 4, Supporting Information Table 3). Some of these enriched biological processes such as ribosomal biogenesis, organelle fission, and some mRNA processing are understood processes controlled by mTORC1. However, several processes dealing with RNA regulation, including transcriptional regulation are more poorly understood and represent a new line of inquiry to understand these aspects of acute resveratrol treatment under serum-deprived conditions.

We also examined protein phosphorylation sites showing the strongest regulation by resveratrol (sites induced or reduced greater than 2.8-fold (Table 1)). We noticed that several of the sites showing the strongest regulation were involved in mTORC1/S6K signaling including PRAS40, Elongation factor Tu GTP-binding domain-containing protein 2, and Tousled-like kinase 2 which was recently found to be associated with the

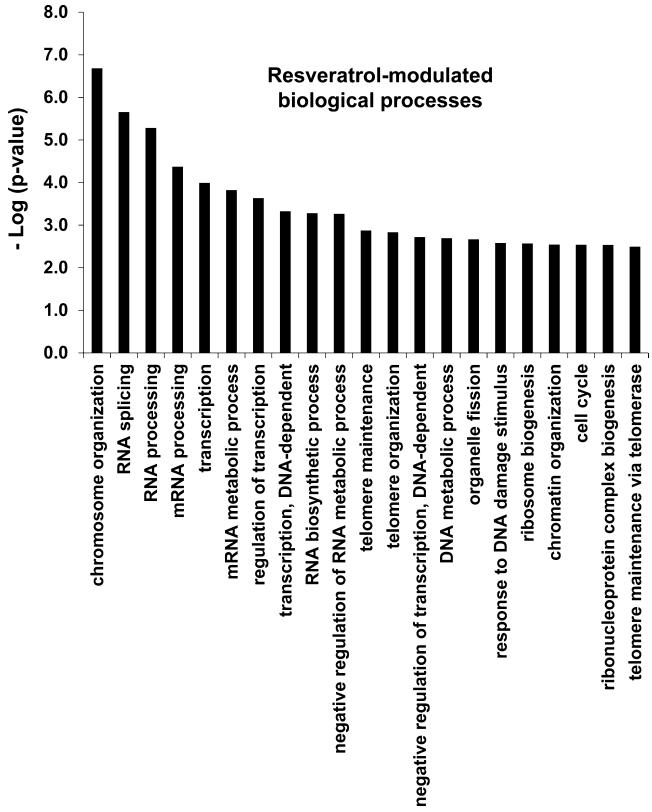

Figure 4. Gene Ontology enrichment demonstrates Resveratrol action affects multiple biological processes. The DAVID bioinformatics resource was utilized to generate enriched biological processes utilizing gene lists generated from ±1 standard deviation from the mean of the quantification value at the protein level. (The quantification from the same site identified from multiple peptides was averaged; however, any significance in a greater number of peptide identifications was not taken into account for weighting here.) A cutoff of $-\log(p\text{-value}) > 2.5$ was employed to only include highly enriched terms.

negative regulation of amino acid starvation-induced autophagy.[39] Among these strongly regulated sites were also regulators of transcription including apoptosis antagonizing transcription factor (AATF), Forkhead box protein A1 (FOXA1) and p53. Of note is the observed resveratrol-dependent induction in the phosphorylation of the tumor suppressor and transcription factor, p53 at Ser392 (Table 1). Increased phosphorylation at this site has the documented role of activating the transcriptional activity of the protein *in vivo*.[40] Moreover, the quantitative change comes in line with previous work demonstrating that the energy-dependent localization of p53 to the nucleus requires regions within the p53 carboxyl-terminus, including phosphorylation at Ser392.[41] Also representing resveratrol's modulation of transcription, we observed a resveratrol-dependent increase in the phosphorylation of the histone deacetylase, HDAC1, at both Ser421 and Ser423 sites, which promotes HDAC enzymatic activity.[42] Interestingly, AATF whose phosphorylation is negatively regulated by resveratrol is a modulator of HDAC1, preventing HDAC1 association with the tumor suppressor Rb.[43] Finally, another cell cycle modulator/transcriptional regulator was identified, cyclin-dependent kinase 12 (CDC12), to be resveratrol-regulated. In this case, resveratrol induces a reduction in phosphorylation of a singly phosphorylated (S681) peptide and a coincident increase in a doubly

dx.doi.org/10.1021/pr500714a | J. Proteome Res. 2014, 13, 5734−5742

Table 1. Phosphopeptides showing Log2 SILAC H/L ratio greater than or equal to ±1.5 (~2.8 fold higher or lower following resveratrol treatement)[a]

gene symbol	protein name	site 1	site 2	site 3	resveratrol-induced fold change
AATF	Apoptosis antagonizing transcription factor	316	320	321	↓3.23
AFF4	ALL1 fused gene from 5q31 family mem. 4	836			↓9.50
AHSG	Alpha-2-HS-glycoprotein chain B	204			↑25.00
AKT1S1 (PRAS40)	Proline-rich AKT1 substrate 1	266 (246)			↓13.84
AKT1S1 (PRAS40)	Proline-rich AKT1 substrate 1	203 (183)			↓8.83
CRKRS (CDK12)	Cdc2-related kinase	681	685		↑1.10
CRKRS (CDK12)	Cdc2-related kinase	681			↓5.00
EFTUD2	Elongation factor Tu GTP-binding domain-containing protein 2	86			↑3.13
ERC2	ELKS/RAB6-interact./CAST family mem. 2	585	591		↓10.02
FOXA1	Forkhead box protein A1	302			↑3.33
FOXA1	Forkhead box protein A1	308			↑1.32
ITPR3	Inositol 1,4,5-triphosphate receptor, type 3	934			↑1.92
NCAPH	Non-SMC condensin I complex subunit H	432			↑5.56
NKX1-2	NK1 transcription factor-rel. protein 2	60			↑8.33
PHF14	PHD finger protein 14	287	290		↑2.86
PLXDC2	Plexin domain containing 2	506			↑3.03
RFX2	DNA binding regulatory factor X 2	652	654	656	↑7.14
TLK2	Tousled-like kinase 2	749			↑3.03
TMPO	Thymopoietin	351			↓10.92
TP53	Tumor protein p53	392			↑2.78
ZC3HAV1	CCCH-type zinc finger antiviral protein	675			↑14.29

[a]Indicated are gene symbol (with hyperlink to protein page at PhosphositePlus), protein name, phosphorylation site numbers and resveratrol-induced fold change (see Supporting Information Table 4 for additional information).

phosphorylated peptide (S681 and S685; Table 1). The function of this phosphorylation is not known.

Given our current understanding, these data suggest that resveratrol's mechanism of action on mTORC1 signaling might be predominately mediated by reducing phosphorylation of PRAS40 at T246 and S183. Reducing PRAS40 T246 and S183 phosphorylation would increase PRAS40's binding to RAPTOR/TORC1. This would then competitively reduce 4E-BP1 binding to mTORC1.[34] 4E-BP1 is thought to be nearly maximally phosphorylated under serum-starved conditions[34] and yet we did observe resveratrol-dependent reduction in 4E-BP1 pSer65 phosphorylation and/or electrophoretic mobility (Figure 3). It is unclear then if eIF4E might still be able to proceed with 5′ cap-dependent translation (Figure 5) in serum-starved, resveratrol-treated cells. This is a subject of our future studies. The exact mechanism by which the reduction in PRAS40 phosphorylation might participate in protection from autophagy remains unclear and it is formally possible that mTORC1 is not involved at all. However, one possibility is that the interaction with the 14-3-3 proteins may play a role. 14-3-3 proteins have been reported to regulate autophagosome formation,[33] and serum starvation-induced dissociation of 14-3-3 proteins from PRAS40 would affect the ability of PRAS40 to signal to mTORC1, causing autophagy induction. There is already evidence for the role of 14-3-3 in autophagy.[44] Additionally, an emerging question is how resveratrol might reduce PRAS40 phosphorylation. Given that our treatment with resveratrol was under serum-starved conditions, our data suggest the presence of some basal Akt activity toward PRAS40 that remains in the starved state, and that this basal activity is inhibited by resveratrol. Alternatively, resveratrol might be activating a PRAS40 phosphatase or as mentioned above, resveratrol might be inhibiting another AGC kinase with basal

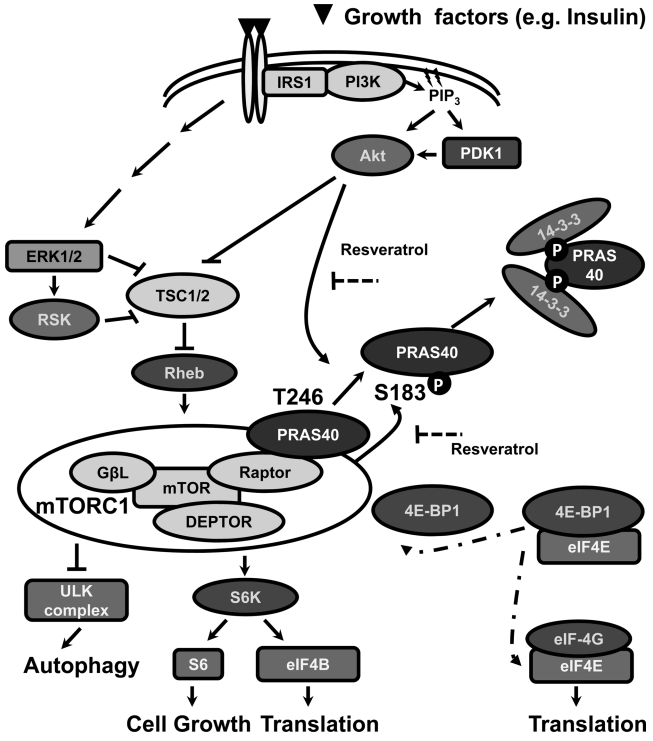

Figure 5. Schematic representation of the PI3K/mTOR signaling pathway upon stimulation with growth factors, with an emphasis on the phosphoregulation of PRAS40.

dx.doi.org/10.1021/pr500714a | J. Proteome Res. 2014, 13, 5734−5742

activity toward PRAS40. These questions will be the subject of important future studies, as will be the mechanisms by which resveratrol regulates the transcriptional and cell cycle events discussed herein.

Upregulation of autophagy may be responsible for protecting cancer cells against apoptosis. Importantly, in this study we showed that resveratrol is able to prevent induction of markers of autophagy, a process which may promote progression to apoptosis.[5] Because resveratrol is a widely available oral natural supplement with a low toxicity profile, further studies would focus on its potential therapeutic use in cancer treatment, especially in combination with other agents.

■ ASSOCIATED CONTENT

Supporting Information

Normal quantile plots of SILAC ratio distributions (H/L) of MCF-7-derived phosphopeptides and phosphoproteins; phosphopeptides identified from SILAC labeled, serum-starved MCF7 cells differentially treated with resveratrol (heavy); phosphopeptides without heavy lysine residues identified from SILAC labeled, serum-starved MCF7 cells differentially treated with resveratrol (heavy); biological processes modified by resveratrol treatment as identified by Gene Ontology biological processes; phosphopeptides showing Log2 SILAC H/L ratio greater than or equal to ±1.5. This material is available free of charge via the Internet at http://pubs.acs.org.

■ AUTHOR INFORMATION

Corresponding Authors

*E-mail: bballif@uvm.edu.
*E-mail: mholz@yu.edu.

Author Contributions

⊥A.A. and P.F.D. contributed equally.

Notes

The authors declare no competing financial interest.

■ ACKNOWLEDGMENTS

This work was supported by grants to M.K.H. from the NIH (CA151112), the Atol Charitable Trust, the LAM Foundation (098P0113), and the American Cancer Society (RSG-13-287-01-TBE). Fellowship support to A.A. was from the National Cancer Center. Additional funding came from Yeshiva University and the University of Vermont. Proteomics analyses were supported by the Vermont Genetics Network (NIH NIGMS/INBRE 8P20GM103449).

■ REFERENCES

(1) Blagosklonny, M. V. An anti-aging drug today: From senescence-promoting genes to anti-aging pill. *Drug Discovery Today* **2007**, *12* (5−6), 218−24.

(2) Howitz, K. T.; Bitterman, K. J.; Cohen, H. Y.; Lamming, D. W.; Lavu, S.; Wood, J. G.; Zipkin, R. E.; Chung, P.; Kisielewski, A.; Zhang, L. L.; Scherer, B.; Sinclair, D. A. Small molecule activators of sirtuins extend Saccharomyces cerevisiae lifespan. *Nature* **2003**, *425* (6954), 191−6.

(3) Baur, J. A.; Pearson, K. J.; Price, N. L.; Jamieson, H. A.; Lerin, C.; Kalra, A.; Prabhu, V. V.; Allard, J. S.; Lopez-Lluch, G.; Lewis, K.; Pistell, P. J.; Poosala, S.; Becker, K. G.; Boss, O.; Gwinn, D.; Wang, M.; Ramaswamy, S.; Fishbein, K. W.; Spencer, R. G.; Lakatta, E. G.; Le Couteur, D.; Shaw, R. J.; Navas, P.; Puigserver, P.; Ingram, D. K.; de Cabo, R.; Sinclair, D. A. Resveratrol improves health and survival of mice on a high-calorie diet. *Nature* **2006**, *444* (7117), 337−42.

(4) Armour, S. M.; Baur, J. A.; Hsieh, S. N.; Land-Bracha, A.; Thomas, S. M.; Sinclair, D. A. Inhibition of mammalian S6 kinase by resveratrol suppresses autophagy. *Aging* **2009**, *1* (6), 515−28.

(5) Alayev, A.; Sun, Y.; Snyder, R. B.; Berger, S. M.; Yu, J. J.; Holz, M. K. Resveratrol prevents rapamycin-induced upregulation of autophagy and selectively induces apoptosis in TSC2-deficient cells. *Cell Cycle* **2014**, *13* (3), 371−82.

(6) Shintani, T.; Klionsky, D. J. Autophagy in health and disease: A double-edged sword. *Science* **2004**, *306* (5698), 990−5.

(7) Loewith, R.; Jacinto, E.; Wullschleger, S.; Lorberg, A.; Crespo, J. L.; Bonenfant, D.; Oppliger, W.; Jenoe, P.; Hall, M. N. Two TOR complexes, only one of which is rapamycin sensitive, have distinct roles in cell growth control. *Mol. Cell* **2002**, *10* (3), 457−68.

(8) Alayev, A.; Holz, M. K. mTOR signaling for biological control and cancer. *J. Cell Physiol.* **2013**, *228* (8), 1658−64.

(9) Kim, S. G.; Buel, G. R.; Blenis, J. Nutrient regulation of the mTOR complex 1 signaling pathway. *Mol. Cells* **2013**, *35* (6), 463−73.

(10) Buel, G. R.; Kim, S. G.; Blenis, J. mTORC1 signaling aids in CADalyzing pyrimidine biosynthesis. *Cell Metab.* **2013**, *17* (5), 633−5.

(11) Cota, D.; Proulx, K.; Smith, K. A.; Kozma, S. C.; Thomas, G.; Woods, S. C.; Seeley, R. J. Hypothalamic mTOR signaling regulates food intake. *Science* **2006**, *312* (5775), 927−30.

(12) Peng, T.; Golub, T. R.; Sabatini, D. M. The immunosuppressant rapamycin mimics a starvation-like signal distinct from amino acid and glucose deprivation. *Mol. Cell. Biol.* **2002**, *22* (15), 5575−84.

(13) Jang, M.; Cai, L.; Udeani, G. O.; Slowing, K. V.; Thomas, C. F.; Beecher, C. W.; Fong, H. H.; Farnsworth, N. R.; Kinghorn, A. D.; Mehta, R. G.; Moon, R. C.; Pezzuto, J. M. Cancer chemopreventive activity of resveratrol, a natural product derived from grapes. *Science* **1997**, *275* (5297), 218−20.

(14) Goswami, T.; Ballif, B. A. Methods for the isolation of phosphoproteins and phosphopeptides for mass spectrometry analysis: Toward increased functional phosphoproteomics. In *Sample Preparation in Biological Mass Spectrometry*; Ivanov, A. R., Lazarev, A. V., Eds; Springer: New York, NY, 2011; pp 627−655.

(15) Dephoure, N.; Gygi, S. P. A solid phase extraction-based platform for rapid phosphoproteomic analysis. *Methods* **2011**, *54* (4), 379−86.

(16) Elias, J. E.; Gygi, S. P. Target-decoy search strategy for mass spectrometry-based proteomics. *Methods Mol. Biol.* **2010**, *604*, 55−71.

(17) Matsuoka, S.; Ballif, B. A.; Smogorzewska, A.; McDonald, E. R., 3rd; Hurov, K. E.; Luo, J.; Bakalarski, C. E.; Zhao, Z.; Solimini, N.; Lerenthal, Y.; Shiloh, Y.; Gygi, S. P.; Elledge, S. J. ATM and ATR substrate analysis reveals extensive protein networks responsive to DNA damage. *Science* **2007**, *316* (5828), 1160−6.

(18) Bakalarski, C. E.; Elias, J. E.; Villen, J.; Haas, W.; Gerber, S. A.; Everley, P. A.; Gygi, S. P. The impact of peptide abundance and dynamic range on stable-isotope-based quantitative proteomic analyses. *J. Proteome Res.* **2008**, *7* (11), 4756−65.

(19) Huttlin, E. L.; Jedrychowski, M. P.; Elias, J. E.; Goswami, T.; Rad, R.; Beausoleil, S. A.; Villen, J.; Haas, W.; Sowa, M. E.; Gygi, S. P. A tissue-specific atlas of mouse protein phosphorylation and expression. *Cell* **2010**, *143* (7), 1174−89.

(20) Beausoleil, S. A.; Villen, J.; Gerber, S. A.; Rush, J.; Gygi, S. P. A probability-based approach for high-throughput protein phosphorylation analysis and site localization. *Nat. Biotechnol.* **2006**, *24* (10), 1285−92.

(21) Huang da, W.; Sherman, B. T.; Lempicki, R. A. Systematic and integrative analysis of large gene lists using DAVID bioinformatics resources. *Nat. Protoc.* **2009**, *4* (1), 44−57.

(22) Huang da, W.; Sherman, B. T.; Lempicki, R. A. Bioinformatics enrichment tools: paths toward the comprehensive functional analysis of large gene lists. *Nucleic Acids Res.* **2009**, *37* (1), 1−13.

(23) Yamnik, R. L.; Digilova, A.; Davis, D. C.; Brodt, Z. N.; Murphy, C. J.; Holz, M. K. S6 kinase 1 regulates estrogen receptor alpha in control of breast cancer cell proliferation. *J. Biol. Chem.* **2009**, *284* (10), 6361−9.

(24) Ichimura, Y.; Kominami, E.; Tanaka, K.; Komatsu, M. Selective turnover of p62/A170/SQSTM1 by autophagy. *Autophagy* **2008**, *4* (8), 1063−6.
(25) Alayev, A.; Berger, S. M.; Kramer, M. Y.; Schwartz, N. S.; Holz, M. K. The combination of rapamycin and resveratrol blocks autophagy and induces apoptosis in breast cancer cells. *J. Cell. Biochem.* **2014**, DOI: 10.1002/jcb.24997.
(26) Ong, S. E.; Blagoev, B.; Kratchmarova, I.; Kristensen, D. B.; Steen, H.; Pandey, A.; Mann, M. Stable isotope labeling by amino acids in cell culture, SILAC, as a simple and accurate approach to expression proteomics. *Mol. Cell Proteomics* **2002**, *1* (5), 376−86.
(27) Doubleday, P.; Ballif, B. Developmentally-dynamic murine brain proteomes and phosphoproteomes revealed by quantitative proteomics. *Proteomes* **2014**, *2* (2), 191−207.
(28) Sefton, B. M.; Hunter, T.; Beemon, K.; Eckhart, W. Evidence that the phosphorylation of tyrosine is essential for cellular transformation by Rous sarcoma virus. *Cell* **1980**, *20* (3), 807−16.
(29) Olsen, J. V.; Blagoev, B.; Gnad, F.; Macek, B.; Kumar, C.; Mortensen, P.; Mann, M. Global, in vivo, and site-specific phosphorylation dynamics in signaling networks. *Cell* **2006**, *127* (3), 635−48.
(30) Lee, S. B.; Kim, S.; Lee, J.; Park, J.; Lee, G.; Kim, Y.; Kim, J. M.; Chung, J. ATG1, an autophagy regulator, inhibits cell growth by negatively regulating S6 kinase. *Embo Rep.* **2007**, *8* (4), 360−5.
(31) Shang, L.; Chen, S.; Du, F.; Li, S.; Zhao, L.; Wang, X. Nutrient starvation elicits an acute autophagic response mediated by Ulk1 dephosphorylation and its subsequent dissociation from AMPK. *Proc. Natl. Acad. Sci. U.S.A.* **2011**, *108* (12), 4788−93.
(32) Nascimento, E. B.; Snel, M.; Guigas, B.; van der Zon, G. C.; Kriek, J.; Maassen, J. A.; Jazet, I. M.; Diamant, M.; Ouwens, D. M. Phosphorylation of PRAS40 on Thr246 by PKB/AKT facilitates efficient phosphorylation of Ser183 by mTORC1. *Cell Signalling* **2010**, *22* (6), 961−7.
(33) Kovacina, K. S.; Park, G. Y.; Bae, S. S.; Guzzetta, A. W.; Schaefer, E.; Birnbaum, M. J.; Roth, R. A. Identification of a proline-rich Akt substrate as a 14-3-3 binding partner. *J. Biol. Chem.* **2003**, *278* (12), 10189−94.
(34) Rapley, J.; Oshiro, N.; Ortiz-Vega, S.; Avruch, J. The mechanism of insulin-stimulated 4E-BP protein binding to mammalian target of rapamycin (mTOR) complex 1 and its contribution to mTOR complex 1 signaling. *J. Biol. Chem.* **2011**, *286* (44), 38043−53.
(35) Schalm, S. S.; Fingar, D. C.; Sabatini, D. M.; Blenis, J. TOS motif-mediated raptor binding regulates 4E-BP1 multisite phosphorylation and function. *Curr. Biol.* **2003**, *13* (10), 797−806.
(36) Holz, M. K.; Ballif, B. A.; Gygi, S. P.; Blenis, J. mTOR and S6K1 mediate assembly of the translation preinitiation complex through dynamic protein interchange and ordered phosphorylation events. *Cell* **2005**, *123* (4), 569−80.
(37) Frojdo, S.; Cozzone, D.; Vidal, H.; Pirola, L. Resveratrol is a class IA phosphoinositide 3-kinase inhibitor. *Biochem. J.* **2007**, *406* (3), 511−8.
(38) Casamayor, A.; Morrice, N. A.; Alessi, D. R. Phosphorylation of Ser-241 is essential for the activity of 3-phosphoinositide-dependent protein kinase-1: Identification of five sites of phosphorylation in vivo. *Biochem. J.* **1999**, *342* (Pt 2), 287−92.
(39) McKnight, N. C.; Jefferies, H. B.; Alemu, E. A.; Saunders, R. E.; Howell, M.; Johansen, T.; Tooze, S. A. Genome-wide siRNA screen reveals amino acid starvation-induced autophagy requires SCOC and WAC. *EMBO J.* **2012**, *31* (8), 1931−46.
(40) Hao, M.; Lowy, A. M.; Kapoor, M.; Deffie, A.; Liu, G.; Lozano, G. Mutation of phosphoserine 389 affects p53 function in vivo. *J. Biol. Chem.* **1996**, *271* (46), 29380−5.
(41) Karni-Schmidt, O.; Friedler, A.; Zupnick, A.; McKinney, K.; Mattia, M.; Beckerman, R.; Bouvet, P.; Sheetz, M.; Fersht, A.; Prives, C. Energy-dependent nucleolar localization of p53 in vitro requires two discrete regions within the p53 carboxyl terminus. *Oncogene* **2007**, *26* (26), 3878−91.
(42) Pflum, M. K.; Tong, J. K.; Lane, W. S.; Schreiber, S. L. Histone deacetylase 1 phosphorylation promotes enzymatic activity and complex formation. *J. Biol. Chem.* **2001**, *276* (50), 47733−41.
(43) Bruno, T.; De Angelis, R.; De Nicola, F.; Barbato, C.; Di Padova, M.; Corbi, N.; Libri, V.; Benassi, B.; Mattei, E.; Chersi, A.; Soddu, S.; Floridi, A.; Passananti, C.; Fanciulli, M. Che-1 affects cell growth by interfering with the recruitment of HDAC1 by Rb. *Cancer Cell* **2002**, *2* (5), 387−99.
(44) Pozuelo-Rubio, M. 14−3-3 Proteins are regulators of autophagy. *Cells* **2012**, *1* (4), 754−73.